Widths of atomic M-shell vacancy states and quasiatomic aspects of radiationless transitions in solids

Lo I Yin and Isidore Adler
NASA—Goddard Space Flight Center, Code 641, Greenbelt, Maryland 20771

Tung Tsang
Department of Physics, Howard University, Washington, D.C. 20001

Mau Hsiung Chen, Douglas A. Ringers, and Bernd Crasemann
*Department of Physics, University of Oregon, Eugene, Oregon 97403**
(Received 25 October 1973)

Widths of M-level vacancy states in atoms with $29 \leq Z \leq 48$ have been measured by x-ray photoelectron spectroscopy. The results are consistently smaller, sometimes by a factor of ≥ 3, than expected from previous theory, and do not show the pronounced effect of predicted "super-Coster-Kronig" transitions. The Cu and Zn L_3-$M_{4,5}M_{4,5}$ Auger and $M_{4,5}$ photoelectron spectra have been measured; the Auger spectra exhibit characteristics of free-atom spectra and do not reflect the structure of the band from which the M electrons originate. Drawing upon this and other evidence suggesting that atoms in solids can behave as quasifree when undergoing radiationless transitions, free-atom M Auger and Coster-Kronig energies have been computed. These are smaller than measured energies because the effect of extra-atomic relaxation is absent. M-level widths were calculated with these energies, in a neutral-atom potential. Good agreement with experiment is attained.

I. INTRODUCTION

Very little experimental information on the lifetimes of atomic M-shell vacancies is available; only at high Z have some x-ray coincidence experiments been possible.[1] At medium Z, isolated studies of Auger and x-ray linewidths have been performed.[2-5] However, these linewidths are the sums of initial- and final-state widths, and information on L- and N-level widths is also scarce. On the other hand, the photoelectron linewidth in x-ray photoelectron spectroscopy (XPS) directly reflects the width of the atomic vacancy state that is produced; only the width of the incident x ray and instrumental broadening need to be accounted for. When the instrumental width is made negligible and the x-ray width is constant and known, a direct determination of atomic-level widths is possible by XPS.

In general, the width of a vacancy state is the sum of radiative, Auger, and Coster-Kronig widths:

$$\Gamma = \Gamma_R + \Gamma_A + \Gamma_{CK} . \tag{1}$$

For the M shells in the medium-Z region, with which the present study is concerned, several simplifying conditions apply.

(i) Radiative transition rates are so small (M-shell fluorescence yields being well below 1%) that the lifetime of an M vacancy is almost entirely determined by Auger and Coster-Kronig decay.

(ii) For the M_1 and $M_{2,3}$ ($3s, 3p$) subshells, Coster-Kronig transitions are energetically possible and are so intense that virtually the entire width is due to them.

(iii) For the $M_{4,5}$ ($3d$) subshells, Coster-Kronig transitions are absent, and the total width is almost entirely due to Auger transitions.

Measurements of the width of M-shell vacancy states therefore constitute, in essence, direct measurements of the dominant Auger or Coster-Kronig rates. Such measurements are of particular interest at the present time because of recent theoretical work on the subject.[6-9] In particular, McGuire's comprehensive calculations[6,7] of M-shell Auger and Coster-Kronig rates predict the existence of very intense M_i-M_jM_k ("super-Coster-Kronig") transitions. These super-Coster-Kronig transitions are only possible for $Z \leq 36$; hence the M_2 and M_3 subshell widths are expected to drop sharply at $Z = 36$.

In Secs. II A and II B we describe XPS measurements of M-level widths, and in Sec. II C we identify substantial discrepancies between measured M-vacancy lifetimes and those predicted in previous calculations.[6,7] In Sec. III, we describe experiments on the Auger and photoelectron spectra of Cu and Zn; the observed L_3-$M_{4,5}M_{4,5}$ Auger spectra of these elements exhibit distinct

characteristics of free-atom spectra and do not reflect the structure of the band from which the M electrons originate. Drawing upon this and other evidence suggesting that atoms in solids can behave as quasifree when undergoing radiationless transitions, we compute *free-atom M* Auger and Coster-Kronig energies and calculate the widths of M vacancy states from these energies, in a neutral-atom potential (Sec. IV). The theoretical widths derived in this manner agree well with the measurements.

II. WIDTHS OF M-SUBSHELL VACANCY STATES: EXPERIMENTS

A. Measurements

The XPS assembly, described previously,[10] is operated in an oil-free vacuum of $\sim 1\times 10^{-8}$ Torr. Aluminum $K\alpha_{1,2}$ x rays were used for excitation. Photoelectrons were analyzed in a hemispherical electrostatic spectrometer of 11-cm radius. To achieve high resolution, photoelectrons were retarded to ~60 eV before entering the spectrometer. Electrons were pulse-counted and their energy distribution was recorded with a multichannel analyzer operated in the multiscaler mode.

Samples consisted of spectroscopically pure foils, except for Ge, which was vacuum-deposited on Cu. The sample surfaces were sputter-cleaned in an antechamber with Ar ions at 1.5 kV, 0.2 mA/cm^2, 20 μm pressure. Approximately 6 min elapsed between the end of ion sputtering and the beginning of analysis at 5×10^{-8} Torr.

For the level-width measurements, the absolute resolution of the spectrometer was progressively improved, at the expense of intensity, by reducing the energy of electrons entering the spectrometer. The full width at half-maximum (FWHM) of the Al $K\alpha_{1,2}$-excited $N_7(4f_{7/2})$ photoelectron line of Au then decreased to a minimum of 1.31 eV; additional improvement of the spectrometer resolution had no further effect. It thus appears that, at such spectrometer settings, the instrumental contribution to the measured photoelectron line width is negligible—at least for lines considerably wider than 1.3 eV (Sec. II B). To ascertain re-

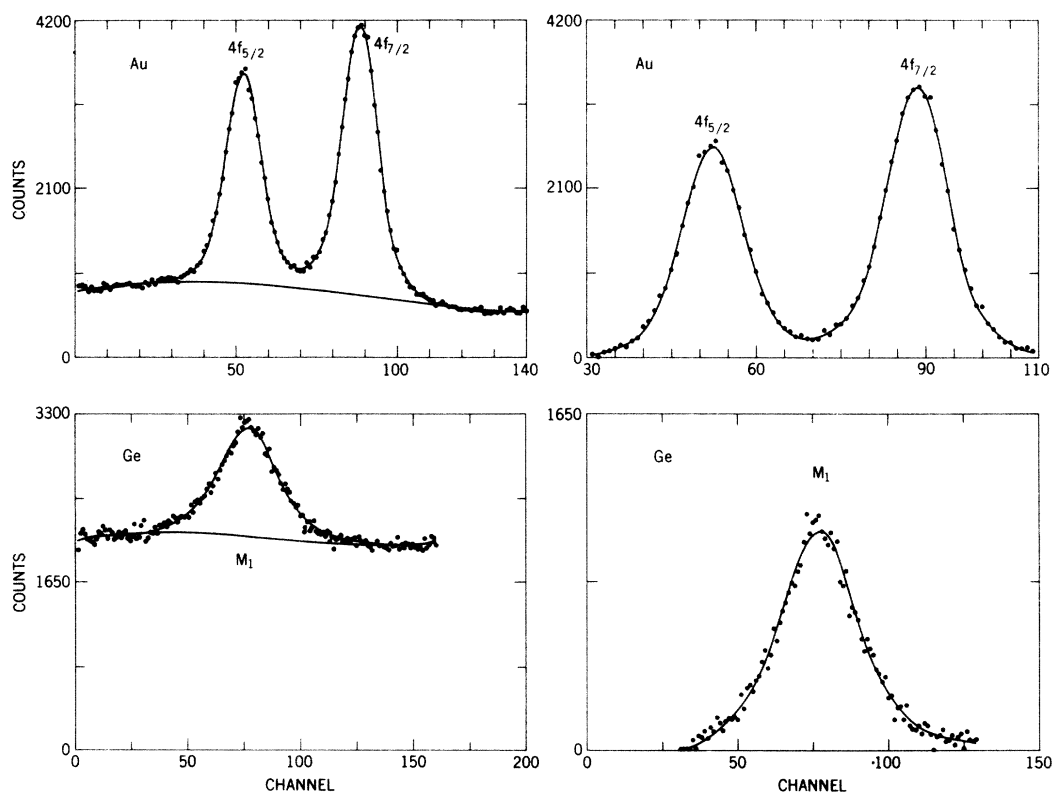

FIG. 1. CalComp plots of measured electron spectra, illustrating smoothing by a spline-fitted computer program and background generated by fourth-degree polynomials. Top: Al $K\alpha_{1,2}$-excited photoelectron spectrum of the N_6 and N_7 ($4f_{5/2}, 4f_{7/2}$) doublet of Au. Bottom: Al $K\alpha_{1,2}$-excited photoelectron line of the M_1 (3s) level of Ge. Left-hand side: Prior to background subtraction. Right-hand side: after background subtraction. FWHM of the Au N_7 line is 1.31 eV, and of the Ge M_1 line, 2.9 eV. Units on the abscissa are 0.1 eV per channel.

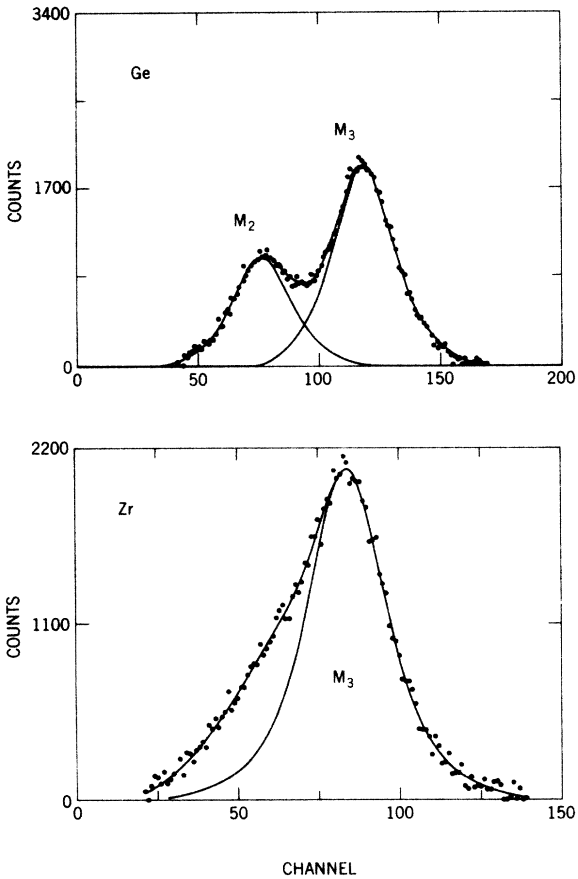

FIG. 2. Top: photoelectron spectrum of the M_2 and M_3 levels of Ge. The peaks are resolved by a DuPont 310 curve resolver. Bottom: photoelectron spectrum of the M_3 level of Zr, showing the effect of chemical contamination on the left (high binding-energy) side of the peak. An artificial symmetric peak is constructed to measure the line width. Units on the abscissa are 0.1 eV per channel.

producibility, each level width was measured at least twice, with different samples.

B. Data analysis and results

The data were smoothed with a spline-fit computer program; background on both sides of a peak was fitted with a single fourth-degree polynomial. Results were plotted with a CalComp-780 (Fig. 1). When adjacent photoelectron lines were not completely resolved by the electrostatic spectrometer, the background-subtracted smooth spectrum was deconvoluted with a DuPont 310 curve resolver (Fig. 2); in such cases, the errors assigned to the width measurements were appropriately increased.

It is well known that XPS is extremely surface-sensitive. Even with spectroscopically pure sample materials, surface contamination was inevitable. After Ar ion sputtering, the cleanliness of each sample surface was tested by monitoring the 1*s* photoelectron lines of C and O. For most samples, these lines became either nondetectable or barely discernible above background after prolonged ion-sputtering treatment. In these cases, the photoelectron lines of interest have a symmetrical shape (Fig. 1, bottom). However, for a strong getter material like Zr, no amount of ion sputtering eliminated the presence of O and C, indicating a chemically contaminated surface of oxide and carbide. Consequently, asymmetry appears on the low-energy side (high binding energy) of the photoelectron lines of Zr and, to a lesser extent, of Nb. To determine the linewidths in these cases, a symmetrical line was constructed, using the high-energy side of the photoelectron peak as a guide (Fig. 2, bottom).

The measured widths of M-subshell vacancy states listed in Table I were deduced on the assumption that instrumental broadening is negli-

TABLE I. Measured widths $\Gamma(M_i)$ of M_i-subshell vacancy states, compared with theoretical predictions of McGuire (Ref. 6). All widths are in eV.

	$\Gamma(M_1)$		$\Gamma(M_2)$		$\Gamma(M_3)$		$\Gamma(M_4)$		$\Gamma(M_5)$
	Measured	Predicted	Measured	Predicted	Measured	Predicted	Measured	Predicted	Measured Predicted
$_{29}$Cu	1.9 ± 0.2	6.66	2.0 ± 0.3	5.22	1.6 ± 0.3				
$_{30}$Zn	1.7 ± 0.2	5.90	1.7 ± 0.3	4.70	2.0 ± 0.3				
$_{32}$Ge	2.0 ± 0.2	4.59	2.1 ± 0.2	5.22	2.1 ± 0.2				
$_{40}$Zr	6.0 ± 0.8	6.47	2.2 ± 0.3	2.43	2.0 ± 0.3	2.40	1.0 ± 0.3	0.073	0.6 ± 0.3
$_{41}$Nb	5.8 ± 0.8		1.8 ± 0.2		1.9 ± 0.2		1.1 ± 0.3		0.7 ± 0.3
$_{47}$Ag	8.0 ± 0.8	9.62	2.2 ± 0.15	3.74	2.3 ± 0.15	3.88	$0.3^{+0.15}_{-0.25}$ [a]	0.44	$0.4^{+0.15}_{-0.25}$ [a]
$_{48}$Cd			2.3 ± 0.15		2.5 ± 0.15		$0.4^{+0.15}_{-0.25}$ [a]		$0.5^{+0.15}_{-0.25}$ [a]

[a] The asymmetry of the assigned errors is explained in Sec. II B of the text.

gible, i.e., that the experimental photoelectron linewidth (FWHM) is the Lorentzian sum (simple addition) of the incident x-ray width and the level width. The combined x-ray width of the Al $K\alpha_{1,2}$ lines is taken to be 0.9 eV.[11]

For levels with photoelectron lines considerably wider than 1.3 eV, the assumption of negligible instrumental contribution is welljustified (Sec. II A), and the listed error limits of ±0.15 eV represent a pessimistic estimate of experimental uncertainties, although they do not include possible systematic errors, such as the accuracy of the assumed Al $K\alpha$ x-ray width. The present error limits are larger than those assigned to previous measurements[10] of Cu and Zn L_2 and L_3 widths. To cover a wide range of atomic numbers, it was necessary to compromise somewhat on counting statistics and the number of repetitive runs. Moreover, the signal-to-background ratio is generally much poorer for the wide M_1, M_2, and M_3 lines than for the L_2 and L_3 lines previously studied.

For levels with photoelectron line widths near 1.3 eV, the assigned error was increased to 0.25 eV in the negative direction, to make liberal allowance for the possibility of a (Gaussian) instrumental contribution. For improperly resolved lines, the error estimate includes uncertainties introduced by use of the curve resolver. The large error limits assigned to M_1 level widths for $Z \geq 40$ are due to the fact that these M_1 photoelectron lines are barely above background and very broad.

C. Comparison with previous calculations

A cursory survey of Table I shows that all the observed M_1, M_2, and M_3 level widths are smaller than the first theoretical predictions,[6] some by as much as a factor of ≥3. The discrepancy is all the more significant because, in general, effects such as instrumental contributions, background interference, chemical shifts, and unresolved multiplet splitting tend to *broaden* measured line widths.

1. M_1 level widths

The M_1 widths predicted in Ref. 6 decrease from 6.66 eV for $_{29}$Cu to 5.90 eV for $_{30}$Zn and 4.59 eV for $_{32}$Ge, then increase again for $Z > 36$. The observed widths for these three elements are much smaller (~2 eV) and do not decrease perceptibly

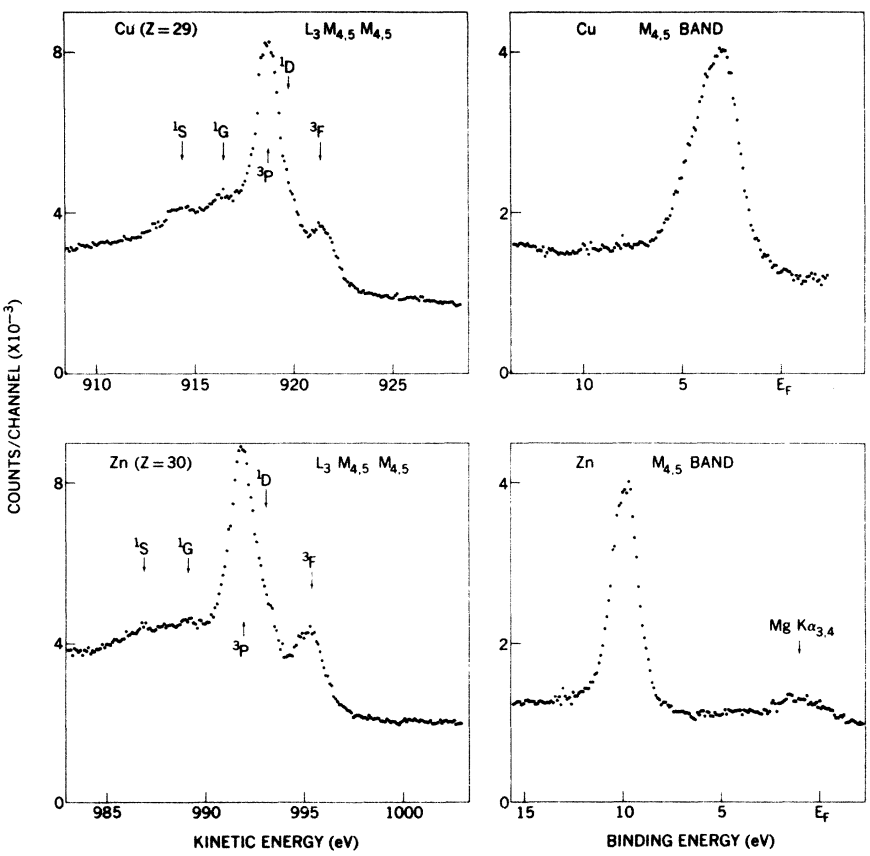

FIG. 3. L_3-$M_{4,5}M_{4,5}$ Auger spectra (left-hand side) and Mg $K\alpha_{1,2}$ x-ray excited valence-band photoelectron spectra (right-hand side) of Cu and Zn. The fine-structure features of the Auger spectra are labeled according to pure LS-coupling terms. The valence-band peak is due mainly to $M_{4,5}$ photoelectrons.

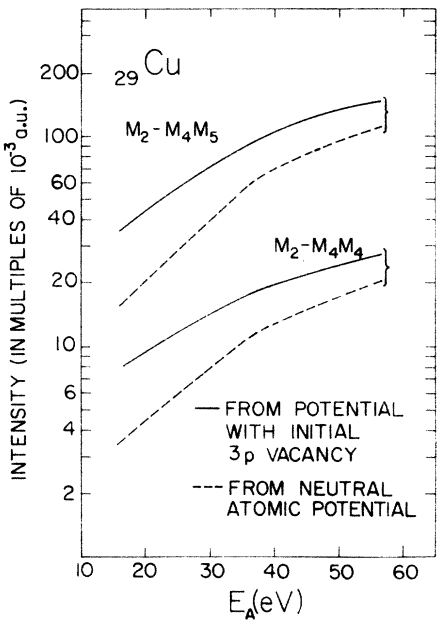

FIG. 4. M_2-M_4M_5 and M_2-M_4M_4 super-Coster-Kronig transition probabilities in Cu, as a function of continuum-electron energy. The rates were computed from Hartree-Slater wave functions with Slater exchange, for two different atomic potentials: (i) in the presence of an M_2 vacancy, (ii) in a neutral atom.

with increasing Z. The widths of these M_1 levels are almost entirely due to Coster-Kronig or super-Coster-Kronig transitions. The energetics suggest that the predicted decrease of M_1 widths with increasing Z would mainly be due to a decrease in super-Coster-Kronig rates. The experimental results imply that (i) the Coster-Kronig transition rates have been overestimated, and (ii) the influence of super-Coster-Kronig rates is not very pronounced, i.e., there is not much difference between Coster-Kronig and super-Coster-Kronig rates in the decay of M_1 vacancies of these elements. For $Z > 40$, measured and predicted M_1 widths and their trend with Z are in better agreement (though experimental errors are larger); here, super-Coster-Kronig transitions are not possible.

2. M_2 and M_3 level widths

For $_{29}$Cu, $_{30}$Zn, and $_{32}$Ge, the M_2 and M_3 photoelectron lines were not quite resolved by the spectrometer. However, in spite of the increased errors, it is clear that these widths are far smaller than predicted.[6] Furthermore, the measured M_2 and M_3 widths of $_{32}$Ge differ little from those of $_{40}$Zr, while the calculations[6] predict a sudden decrease in the M_2 and M_3 widths above $Z = 36$, owing to the cessation of super-Coster-Kronig transitions. We have no measurements for $32 < Z < 40$, hence it is conceivable that the M_2 and M_3 level widths might increase and then suddenly decrease again in this interval, but this seems unlikely because the experimental values do not support the predicted variation with Z for $Z < 32$ nor for $Z > 40$.

In a detailed study of the L x-ray emission spectrum of $_{40}$Zr, Krause *et al.*[5] recently found a width of 5.7 eV for the L_1-$M_{2,3}$ line, for which McGuire's prediction[6, 12, 13] is 10.7 eV. Because our measured Zr M_2 and M_3 widths nearly agree with theory,[6] this discrepancy must be due to theoretical overestimation of the L_1 level width, due to excessive Coster-Kronig rates.

It should be noted that the measured M_2 and M_3 level widths of $_{47}$Ag are wider than those deduced by Parratt[14] (0.6 and 1.3 eV) from L x-ray emission line widths.

3. M_4 and M_5 level widths

The $M_{4,5}$ photoelectrons for elements with $29 \leq Z \leq 32$ appear essentially as a single peak (the d band). No effort was made to resolve them. The M_4 and M_5 lines of $_{40}$Zr and $_{41}$Nb were fairly well-separated, yet not completely resolved. Rather large experimental uncertainties result

TABLE II. Calculated free-atom M_1 Auger-electron energies (in eV).

Element	M_1-M_2N_1	M_1-M_3N_1	M_1-$M_2N_{2,3}$	M_1-$M_3N_{2,3}$	M_1-$M_{4,5}M_{4,5}$	M_1-$M_{4,5}N_1$	M_1-$M_{4,5}N_{2,3}$	M_1-$M_{2,3}M_{4,5}$
$_{22}$Ti	10.2	10.2			33.1	41.2		1.2
$_{23}$V	12.3	12.3			39.2	48.4		2.4
$_{25}$Mn	18.0	18.0			51.7	63.1		6.0
$_{26}$Fe	21.4	21.4			59.1	71.5		8.4
$_{28}$Ni	25.3	25.3			75.0	89.4		10.2
$_{29}$Cu	28.8	28.8			91.0	101.0		18.0
$_{30}$Zn	30.2	30.2			92.0	108.3		13.3
$_{32}$Ge	25.0	32.0	35.0	42.0	91.0	125.0	135.0	
$_{33}$As	26.5	32.5	37.2	43.6	88.4	132.5	143.6	
$_{36}$Kr	29.3	37.0	44.1	51.9	75.4	158.0	173.0	

from this fact and from the problem of chemical contamination. The measured M_4 and M_5 level widths for these two elements are probably on the high side; it has been shown by Krause[14] that the $M\zeta$ (M_5-N_3) x-ray lines have widths of 0.8 and 1.2 eV, respectively, with the N_3 level being the determining one, as testified by $\Gamma(M\zeta) = 9.8$ eV and $\Gamma(M_5) = 0.4$ eV for Ag.

The lines from $_{47}$Ag and $_{48}$Cd were completely separated. For $Z \geq 40$, all M_4 and M_5 photoelectron lines are less than 1.3 eV wide, so that the possibility of instrumental broadening and the accuracy of the assumed Al $K\alpha$ x-ray width become critical. Taking these factors into account, agreement between theory and experiment is reasonably good.

III. QUASIATOMIC L-MM AUGER SPECTRA OF SOLID Cu AND Zn

Resolution of the discrepancies between calculated and measured M-level widths will be shown in Sec. IV to depend upon the fact that atoms in solids, when undergoing Auger transitions, can behave as though they were quasifree. We illustrate this fact by comparing x-ray photoelectron (XPS) and Auger spectra involving the $M_{4,5}$ band electrons of Cu and Zn. Both XPS and soft x-ray emission spectroscopy (SXS) have been used extensively to study the occupied band structure of solids. Off-hand, it might therefore be expected that Auger spectra would also yield band-structure information.[15] Features of K-valence-valence (K-VV) and L-VV Auger spectra have indeed been interpreted in terms of band structure.[16] However, it is not clear whether band-structure information could be derived from recent high-resolution measurements of the L-MM Auger spectrum of Cu.[17,18] We have, therefore, concurrently examined XPS band spectra (excited with Mg $K\alpha_{1,2}$ x rays) and L_3-$M_{4,5}M_{4,5}$ Auger spectra of both Cu and Zn.[19] The results are indicated in Fig. 3. Resolution of the spectrometer was such that the over-all full width at half-maximum of the N_7 photoelectron line of Au was 1.15 eV. The Fermi level (E_F) was established with reference to that of Au.[20]

It is notable that the L_3-$M_{4,5}M_{4,5}$ Auger spectra of Cu and Zn, shown on the left of Fig. 3, are remarkably similar, and do not seem to depend on the band structures of these metals, which are very different as illustrated by the XPS spectra reproduced on the right of Fig. 3. Another important feature is the narrowness of the L_3-$M_{4,5}M_{4,5}$ Auger peaks (~1.2 eV for Cu), which has also been noted by Schön.[18] The width of this Auger group would be expected to include the L_3-level width (0.54 and 0.66 eV for Cu and Zn, respectively[17]) and a self-convolution of the $3d$ density of states (multiplied by the transition probability). The $3d$ bandwidths of Cu and Zn are ~2 eV and ~0.8 eV, respectively, as seen from the XPS $3d$ band spectrum (which includes the Mg $K\alpha_{1,2}$ width of ~0.8 eV and a negligible constant instrumental width). The narrowness of the Auger peak is in sharp contrast to the large observed $L\alpha$ (L_3-$M_{4,5}$) width of Cu and Zn.[21] Furthermore, the L_3-$M_{4,5}M_{4,5}$ Auger lines are seen to be quite symmetrical while the XPS $M_{4,5}$ band peaks are asymmetric.

The fine structure of the Cu and Zn Auger spectra is distinctly similar[17,18] to that of gaseous Kr, and of Br in gaseous bromosubstituted methane.[22] In these gaseous samples, solid-state effects are absent and the L-MM transitions are inner-shell transitions. Furthermore, the fine structure of the Cu and Zn L-MM spectra agrees well with theoretical predictions for pure *atomic* LS-coupling terms of the final-state configuration.[17,23] Similar conclusions regarding other portions of the L-MM spectra have been reached by Powell and Mandl[17] and by Coad.[24]

The aspects enumerated in the preceding paragraphs constitute rather compelling evidence that the L_3-$M_{4,5}M_{4,5}$ Auger spectra of metallic Cu and

TABLE III. Calculated free-atom M_2 and M_3 Auger-electron energies (in eV).

Element	M_2-$M_{4,5}M_{4,5}$	M_2-$M_{4,5}N_1$	M_2-$M_{4,5}N_{2,3}$	M_3-$M_{4,5}M_{4,5}$	M_3-$M_{4,5}N_1$	M_3-$M_{4,5}N_{2,3}$
$_{22}$Ti	8.1	16.2		8.1	16.2	
$_{23}$V	11.2	20.4		11.2	20.4	
$_{25}$Mn	16.7	28.1		16.7	28.1	
$_{26}$Fe	20.1	32.5		20.1	32.5	
$_{28}$Ni	31.0	45.4		31.0	45.4	
$_{29}$Cu	44.0	54.0		44.0	54.0	
$_{30}$Zn	41.0	58.3		41.0	58.3	
$_{32}$Ge	39.4	73.1	83.0	32.4	66.1	76.0
$_{33}$As	31.4	75.5	86.6	25.4	69.5	80.6
$_{36}$Kr	4.2	87.3	102.1		79.5	94.3

TABLE IV. Experimental M Auger-electron energies (Ref. 34) (in eV, with reference to the vacuum).

Element	M_2-$M_{4,5}M_{4,5}$	M_3-$M_{4,5}M_{4,5}$
$_{29}$Cu	56	54
$_{30}$Zn	55	52
$_{32}$Ge	44	41
$_{33}$As	40	35

Zn are "quasiatomic" in character, i.e., that they are essentially free of solid-state band-structure effects. Such quasiatomic characteristics have also been noted by Bassett *et al.*[25] in the K-LL Auger spectra of Mg and O in MgO, by Powell[26] for the $M_{4,5}$-VV spectrum of Ag, and by Wertheim and Rosencwaig[27] in their interpretation of the configuration interaction satellites in the XPS of K in potassium halides.

The quasiatomic characteristics of Auger transitions stand in contrast to the well-established solid-state behavior of SXS. A tentative explanation of this apparent contradiction can be attempted[19] by noting that L_3 photoionization causes the $M_{4,5}(3d)$ electrons to become more tightly bound, owing to a reduction in screening. Consequently, the $3d$ electrons of the ionized atom can be somewhat withdrawn from the band, becoming more localized and behaving more like atomic electrons. The screened Coulomb interaction of the Auger process preferentially selects these localized electrons, thus giving the Auger spectrum its quasiatomic character. The much longer radiative lifetime of the L_3 vacancies, on the other hand, permits time for the reestablishment of band structure through extraatomic relaxation,[28] though the band structure is somewhat distorted, as predicted by Parratt.[29]

TABLE V. Comparison between calculated and measured $_{18}$Ar Auger energies (in eV).

Transition	Energy Theory [a]	Expt. [b]
L_1-L_2M_1	29.4	29.6
L_1-L_3M_1	31.5	
L_1-$L_2M_{2,3}$	47.0	45.8
L_1-$L_3M_{2,3}$	45.1	
L_1-$M_1M_{2,3}$	268.3	268.0
L_2-M_1M_1	177.8	179.9
L_2-$M_1M_{2,3}$	192.6	192.0
L_3-$M_{2,3}M_{2,3}$	204.7	204.2
L_3-$M_1M_{2,3}$	190.5	189.9

[a] This work.
[b] Reference 36.

TABLE VI. Comparison of calculated and measured $_{36}$Kr Auger energies (in eV).

Transition	Theory Larkins [a]	This work	Expt. [b]
L_2-$M_{4,5}M_{4,5}$		1513.5	1513.2
L_3-$M_{4,5}M_{4,5}$		1461.0	1460.4
M_4-$N_1N_{2,3}$	41.45	41.7	41.1
M_4-$N_{2,3}N_{2,3}$	58.13	57.0	55.5
M_5-$N_1N_{2,3}$	40.25	40.5	39.9
M_5-$N_{2,3}N_{2,3}$	56.93	55.8	54.2
M_4-N_1N_1	22.05	28.2	32.14
M_5-N_1N_1	20.85	27.0	30.89

[a] Averages of theoretical energies from Ref. 38.
[b] Reference 37.

IV. COMPUTATION OF M-SUBSHELL WIDTHS FOR QUASIFREE ATOMS

Two major discrepancies between theoretical[6] and experimental widths of the M_1, M_2, and M_3 levels of medium-Z elements have been pointed out in Sec. II C: (i) experimental widths are consistently smaller than predicted, sometimes by a factor of 3 or more, and (ii) the predicted effect of super Coster-Kronig transitions is not observed; in particular, the calculated decrease (by a factor of 2) in M_2 and M_3 widths between $Z=32$ and $Z=40$ is not seen. In an effort to resolve these rather large systematic discrepancies between measured and calculated M-subshell widths, we have reexamined two aspects of the theory: the energetics and the atomic potential.

A. Energetics

Radiationless-transition rates are very energy-sensitive, particularly near threshold.[10, 30] In super-Coster-Kronig transitions, the continuum-electron energy is very low—typically, a few tens of eV. How rapidly the transition probability increases with energy is illustrated in Fig. 4 for two typical cases. Clearly, even small energy

TABLE VII. Comparison between calculated and measured energies $E^*(nl, n'l')$ (in eV).

Element	$E^*(3d, 4s)$ Theory	$E^*(3d, 4s)$ Expt. [a]	$E^*(3d, 3d)$ Theory	$E^*(3d, 3d)$ Expt. [a]
$_{22}$Ti	14.85	15.98		
$_{24}$Cr	14.37	15.30	20.63	20.30
$_{25}$Mn	16.88	17.10		
$_{29}$Cu	17.10	17.30	27.20	26.60
$_{30}$Zn	19.71	20.00		

[a] Average energy from optical spectroscopy data, C. E. Moore, *Atomic Energy Levels*, Natl. Bur. Std. (U.S.) Circ. No. 467 (U.S. GPO, Washington, D. C., 1971), Vol. II.

TABLE VIII. Theoretical M_1 Auger and Coster-Kronig transition probabilities (in multiples of 10^{-3} a.u.).

Transition	$_{22}$Ti	$_{23}$V	$_{25}$Mn	$_{26}$Fe	$_{28}$Ni	$_{30}$Zn	$_{32}$Ge	$_{33}$As	$_{36}$Kr
M_1-M_2M_4	0.698	1.240	2.730	3.639	4.879	6.383			
M_1-M_2M_5	0.802	1.130	2.332	3.311	3.632	4.368			
M_1-M_3M_4	1.103	1.605	3.345	4.701	5.334	6.518			
M_1-M_3M_5	1.899	3.137	6.779	9.198	11.687	14.983			
M_1-M_4M_4	0.034	0.096	0.293	0.410	0.674	1.006	1.459	1.793	1.982
M_1-M_4M_5	0.128	0.396	1.326	2.002	3.776	6.038	4.867	4.135	2.600
M_1-M_5M_5	0.083	0.244	0.772	1.116	1.955	3.018	3.406	3.723	3.586
M_1-M_2N_1	11.605	11.036	9.437	8.624	8.272	7.872	14.499	17.393	15.663
M_1-M_3N_1	23.209	22.072	18.875	17.248	16.545	15.743	24.568	30.090	28.276
M_1-M_4N_1	6.160	8.959	13.937	15.926	19.452	4.658	7.821	8.985	10.567
M_1-M_5N_1	9.240	13.439	20.906	23.888	29.178	6.986	11.720	13.477	15.751
M_1-M_2N_2							1.890	4.614	11.496
M_1-M_2N_3							4.968	11.726	27.635
M_1-M_3N_2							4.096	9.991	23.726
M_1-M_3N_3							7.158	17.737	43.444
M_1-M_4N_2							0.183	0.431	1.349
M_1-M_4N_3							0.163	0.357	1.186
M_1-M_5N_2							0.106	0.226	0.771
M_1-M_5N_3							0.414	0.956	3.016
M_1-N_1N_2								0.128	0.557
M_1-N_1N_3								0.256	1.115
M_1-N_2N_3									0.097
M_1-N_3N_3									0.119

differences, such as those arising from extra-atomic relaxation, can have a substantial effect on some radiationless-transition probabilities, and hence, on the lifetimes of vacancies that decay primarily by such transitions.

As pointed out in Sec. I, the M-level widths are mainly determined by Auger and Coster-Kronig rates. Evidence outlined in Sec. III points toward free-atom-like behavior of atoms undergoing Auger transitions, even when these atoms are in a solid. One is led to the expectation that the widths of M-vacancy states might be quasiatomic, i.e., determined by free-atom Auger and Coster-Kronig energies that are lower (by the extra-atomic relaxation energy) than the observed Auger-electron energies. No measurements of such free-atom Auger energies exist, except for noble gases; hence we derived them from theory.

The Auger-electron energy in a transition filling an $n''l''$ vacancy is

$$E_A = E_{n''l''} - E_{nl} - E^*(nl, n'l'), \tag{2}$$

TABLE IX. Theoretical M_2 Auger and Coster-Kronig transition probabilities (in multiples of 10^{-3} a.u.).

Transition	$_{22}$Ti	$_{23}$V	$_{25}$Mn	$_{26}$Fe	$_{28}$Ni	$_{30}$Zn	$_{32}$Ge	$_{33}$As	$_{36}$Kr
M_2-M_4M_4	0.123	0.422	1.580	2.732	6.897	10.785	13.201	10.359	6.214
M_2-M_4M_5	0.666	2.268	8.163	13.020	34.569	53.119	57.250	37.486	8.442
M_2-M_5M_5	0.011	0.044	0.193	0.342	0.855	1.379	1.890	1.725	1.316
M_2-M_4N_1	13.123	17.286	24.762	26.847	26.869	6.338	8.760	10.660	11.995
M_2-M_5N_1	1.653	2.268	3.284	3.674	4.174	0.960	1.432	1.672	2.057
M_2-M_4N_2							1.842	4.214	11.890
M_2-M_4N_3							2.962	7.094	19.588
M_2-M_5N_2							3.046	6.733	18.089
M_2-M_5N_3							0.306	0.694	2.032
M_2-N_1N_2								0.186	0.702
M_2-N_1N_3								0.022	0.107
M_2-N_2N_3									1.277
M_2-N_3N_3									0.033

TABLE X. Theoretical M_3 Auger and Coster-Kronig transition probabilities (in multiples of 10^{-3} a.u.).

Transition	$_{22}$Ti	$_{23}V$	$_{25}$Mn	$_{26}$Fe	$_{28}$Ni	$_{30}$Zn	$_{32}$Ge	$_{33}$As	$_{36}$Kr
M_3-M_4M_4	0.021	0.074	0.290	0.501	1.221	1.965	2.124	2.058	
M_3-M_4M_5	0.461	1.576	5.680	9.063	24.162	37.231	28.713	17.450	
M_3-M_5M_5	0.317	1.083	3.964	6.764	16.913	26.079	22.392	16.148	
M_3-M_4N_1	2.304	3.090	4.447	4.889	5.191	1.210	1.925	2.247	2.712
M_3-M_5N_1	12.472	16.465	23.600	25.632	25.852	6.088	9.714	11.474	13.052
M_3-M_4N_2							0.233	0.543	1.699
M_3-M_4N_3							2.452	5.392	15.272
M_3-M_5N_2							1.649	3.833	11.024
M_3-M_5N_3							4.686	10.592	30.592
M_3-N_1N_2								0.010	0.054
M_3-N_1N_3								0.202	0.806
M_3-N_2N_3									0.723
M_3-N_3N_3									1.138

where $E_{n''l''}$ and E_{nl} are the absolute values of the binding energies of $n''l''$ and nl electrons in a neutral atom, and $E^*(nl, n'l')$ is the ionization potential for the $n'l'$ subshell in the presence of an nl vacancy. Owing to cancellation of most of the extra-atomic relaxation energy, the binding-energy difference $E_{n''l''} - E_{nl}$ for a neutral atom is closely approximated by the corresponding binding-energy difference measured in solids, as listed in the ESCA tables.[2, 3]

We calculate $E^*(nl, n'l')$ from first principles, using Slater's $X\alpha$ approximation to the exchange correlation term in the expression for the statistical total energy.[31-33] In this method, the energy eigenvalues prove to be derivatives of the total energy with respect to occupation numbers. This leads to the concept of the Slater transition state, whereby a difference in total energies can be well approximated by a difference in single-electron eigenvalues.[31-33] Pertinent results of the calculation are listed in Tables II and III. For comparison, available experimental Auger-electron energies[34] are indicated in Table IV. The difference between calculated free-atom Auger electron energies and measured energies is due to the solid-state effect on the latter quantities; for Cu and Zn, this difference agrees well with the extraatomic relaxation energy according to Kowalczyk *et al.*[35]

As a test of our method for the computation of free-atom Auger-electron energies, we calculated those for Ar L-LM and L-MM transitions that have been measured by Mehlhorn[36]; the results are listed in Table V. In Table VI, we compare our calculated Kr Auger-electron energies

TABLE XI. Theoretical widths of M_1-, M_2-, and M_3-vacancy states (in eV).

Element	$\Gamma(M_1)$	$\Gamma(M_2)$	$\Gamma(M_3)$
$_{22}$Ti	1.496	0.424	0.424
$_{23}$V	1.724	0.606	0.606
$_{25}$Mn	2.197	1.034	1.034
$_{26}$Fe	2.451	1.268	1.148
$_{28}$Ni	2.868	1.997	1.996
$_{30}$Zn	2.111	1.975	1.975
$_{32}$Ge	2.376	2.467	2.010
$_{33}$As	3.429	2.200	1.903
$_{36}$Kr	5.250	2.279	2.097

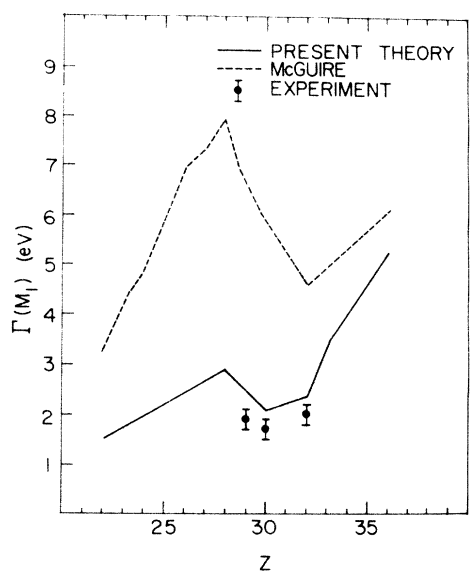

FIG. 5. Radiationless widths (virtually equal to the total widths) of M_1 vacancy states, as a function of atomic number. The widths were computed from Hartree-Slater wave functions with $X\alpha$ exchange in neutral-atom potentials, and are based on theoretical free-atom Auger-electron energies. For comparison, the predictions of McGuire (Refs. 6 and 7) are indicated. Experimental points are from the present x-ray photoelectron spectroscopy measurements of M_1 level widths.

with measurements by Werme *et al.*[37] and intermediate-coupling calculations by Larkins[38] based on Hartree-Fock wave functions. In some cases, it is possible to deduce experimental values of $E^*(nl, n'l')$ from optical spectra; a comparison of such measurements with theoretical values of E^* is indicated in Table VII. In all cases, agreement between theory and experiment is quite satisfactory.

B. Transition rates

To calculate wave functions with which to compute Auger and Coster-Kronig transition probabilities, the Herman-Skillman version[39] of the Hartree-Slater approach was used. The Latter tail correction[40] was included, and $X\alpha$ exchange[31-33] was used, with α values according to Schwarz.[41] Transition rates were computed in j-j coupling in the standard manner.[42-44]

For transition metal atoms, super-Coster-Kronig rates calculated in the potential of an atom with an initial $3p$ vacancy are considerably higher than rates computed in the potential of a neutral atom (Fig. 4). For $_{36}$Kr, on the other hand, the difference in transition probabilities calculated in the two kinds of potentials is less than 10%.

M-shell Auger and Coster-Kronig rates calculated with free-atom continuum-electron energies (Sec. IV A) in the potential of neutral atoms are listed in Tables VIII–X.

C. Comparison of calculated and measured widths

Theoretical widths of M_1, M_2, and M_3 vacancy states are listed in Table XI; these results follow from the transition probabilities indicated in Tables VIII–X. In Fig. 5, the calculated widths of M_1 vacancy states are compared with the results of measurements described in Sec. II. Also indicated are McGuire's[6] predictions, which are based on calculations in the potential of an atom with a $3s$ vacancy, with energies from ESCA measurements[2,3] and the "$Z+1$ rule". Such energies are very close to the observed experimental energies. Similar comparisons of M_2 and M_3 widths are made in Figs. 6 and 7.

It is apparent that satisfactory agreement with experiment can be obtained if (i) radiationless-transition probabilities are calculated for *free-atom energetics*, and (ii) the transition rates are

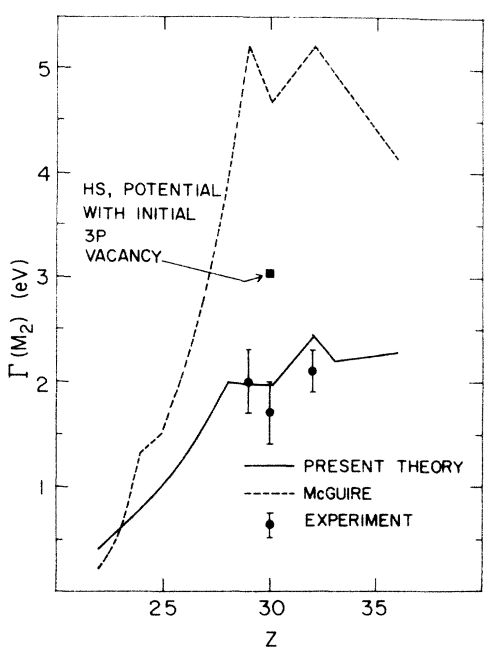

FIG. 6. Radiationless widths (essentially equal to total widths) of M_2 vacancy states, as a function of atomic number. The widths were computed from Hartree-Slater wave functions with $X\alpha$ exchange, in neutral-atom potentials, with calculated free-atom Auger energies; for $_{30}$Zn the result of the calculations is also shown for the potential of an atom with an initial M_2 vacancy. For comparison, the predictions of McGuire (Refs. 6 and 7) are indicated. Experimental widths are from the present x-ray photoelectron spectroscopy measurements.

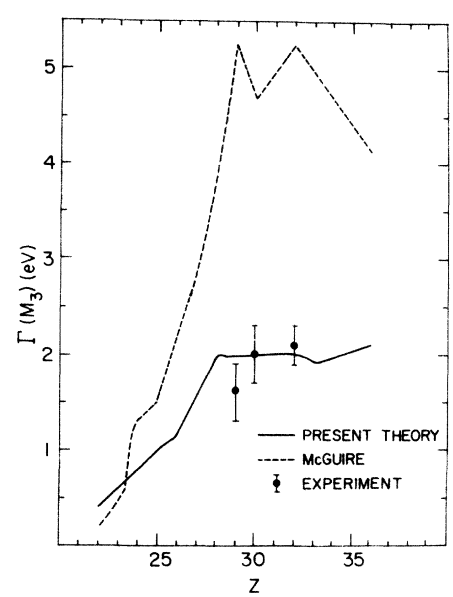

FIG. 7. Radiationless widths (essentially equal to total widths) of M_3 vacancy states, as a function of atomic number. The solid curves were computed from Hartree-Slater wave functions with $X\alpha$ exchange, in neutral-atom potentials, with theoretical free-atom Auger energies. The broken curve represents the calculations of McGuire (Refs. 6 and 7). Data points are results of the present XPS M_3-level width measurements.

computed in the *potential of neutral atoms* (Fig. 6). It can be inferred that the difference between calculated free-atom and measured Auger-electron energies, due to solid-state effects, is imparted to the emerging Auger electron after the atom has undergone the radiationless transition, and further, that the state of the quasiatomic $3d$ electron is better described by the $3d$ wave function of a neutral atom than of an atom with an inner-shell vacancy.

ACKNOWLEDGMENTS

It is a pleasure to acknowledge helpful discussions with A. Temkin and G. D. Mahan. Two of the authors (L. Y. and I. A.) are indebted to E. Fisher for computer programs.

---

*Research supported in part by the U. S. Army Research Office-Durham and by the National Aeronautics and Space Administration (Grant No. NGR-38-003-036).

[1]W. Bambynek, B. Crasemann, R. W. Fink, H.-U. Freund, Hans Mark, C. D. Swift, R. E. Price, and P. Venugopala Rao, Rev. Mod. Phys. 44, 716 (1972).

[2]K. Siegbahn, C. Nordling, G. Johansson, J. Hedman, P. F. Heden, K. Hamrin, U. Gelius, T. Bergmark, L. O. Werme, R. Manne, and Y. Baer, *ESCA Applied to Free Molecules* (North-Holland, Amsterdam, 1969), Chap. IV and Appendix B.

[3]K. Siegbahn, C. Nordling, A. Fahlman, R. Nordberg, K. Hamrin, J. Hedman, G. Johansson, T. Bergmark, S. Karlsson, I. Lindgren, and B. Lindberg, *ESCA, Atomic, Molecular and Solid State Structure Studied by Means of Electron Spectrocopy* (Almqvist and Wiksells, Uppsala, 1967), Chap. VI.

[4]W. Mehlhorn, Z. Phys. 187, 21 (1965).

[5]M. O. Krause, F. Wuilleumier, and C. W. Nestor, Jr., Phys. Rev. A 6, 871 (1972).

[6]E. J. McGuire, Phys. Rev. A 5, 1043 (1972).

[7]E. J. McGuire, Phys. Rev. A 5, 1052 (1972).

[8]C. P. Bhalla, J. Phys. B 3, 916 (1970).

[9]C. P. Bhalla, Phys. Rev. A 6, 1409 (1972).

[10]L. I Yin, I. Adler, M. H. Chen, and B. Crasemann, Phys. Rev. A 7, 897 (1973).

[11]K. Siegbahn, D. Hammond, H. Fellner-Feldegg, and E. F. Barnett, Science 176, 245 (1972).

[12]E. J. McGuire, Phys. Rev. A 3, 587 (1971).

[13]E. J. McGuire, Phys. Rev. A 3, 1801 (1971).

[14]L. G. Parratt, Phys. Rev. 54, 99 (1938); M. O. Krause, Chem. Phys. Lett. 10, 65 (1971).

[15]J. J. Lander, Phys. Rev. 91, 1382 (1953).

[16]R. G. Musket and R. J. Fortner, Phys. Rev. Lett. 26, 80 (1971); G. F. Amelio and E. J. Scheibner, Surface Sci. 11, 242 (1968); Surface Sci. 22, 301 (1970); H. G. Maguire and P. D. Augustus, J. Phys. C 4, L174 (1971); E. N. Sickafus, Phys. Rev. B 7, 5100 (1973).

[17]L. I Yin, T. Tsang, I. Adler, and E. Yellin, J. Appl. Phys. 43, 3464 (1972); C. J. Powell and A. Mandl, Phys. Rev. Lett. 29, 1153 (1972); Phys. Rev. B 6, 4418 (1972).

[18]G. Schön, J. Electron. Spectrosc. 1, 377 (1972/73).

[19]L. I Yin, I. Adler, T. Tsang, M. H. Chen, and B. Crasemann, Phys. Lett. (to be published).

[20]D. A. Shirley, Phys. Rev. B 5, 4709 (1972).

[21]R. J. Liefeld, in *Soft X-Ray Band Spectra,* edited by D. J. Fabian (Academic, New York, 1968), p. 133.

[22]L. O. Werme, T. Bergmark, and K. Siegbahn, Physica Scripta 6, 141 (1972); R. Spohr, T. Bergmark, M. Magnusson, L. O. Werme, and K. Siegbahn, Physica Scripta 2, 31 (1970).

[23]R. E. Watson, Phys. Rev. 118, 1036 (1960); Phys. Rev. 119, 1934 (1960).

[24]J. P. Coad, Phys. Lett. A 37, 437 (1971).

[25]P. J. Bassett, R. E. Gallon, M. Prutton, and J. A. D. Matthew, Surface Sci. 33, 213 (1972).

[26]C. J. Powell, Phys. Rev. Lett. 30, 1179 (1973).

[27]G. K. Wertheim and A. Rosencwaig, Phys. Rev. Lett. 26, 1179 (1971).

[28]D. A. Shirley, Chem. Phys. Lett. 17, 312 (1972); Chem. Phys. Lett. 15, 185 (1972).

[29]L. G. Parratt, Rev. Mod. Phys. 31, 616 (1959).

[30]E. J. Callan, Rev. Mod. Phys. 35, 524 (1963).

[31]J. C. Slater, in *Advances in Quantum Chemistry* edited by P.-O. Lowdin (Academic, New York, 1972), Vol. 6.

[32]J. C. Slater, *Quantum Theory of Molecules and Solids,* Vol. 4: *The Self-Consistent Field for Molecules and Solids* (McGraw-Hill, New York, to be published).

[33]J. C. Slater, J. Phys. Paris 33, C3-1 (1972).

[34]C. C. Chang, Surface Sci. 25, 53 (1971).

[35]S. P. Kowalczyk, R. A. Pollak, F. R. McFeely, L. Ley, and D. A. Shirley, Phys. Rev. B 8, 2387 (1973).

[36]W. Mehlhorn, Z. Phys. 208, 1 (1968).

[37]L. O. Werme, T. Bergmark, and K. Siegbahn, Physica Scripta 6, 141 (1972).

[38]F. P. Larkins, J. Phys. B 6, 1556 (1973).

[39]F. Herman and S. Skillman, *Atomic Structure Calculations* (Prentice-Hall, Englewood Cliffs, N. J., 1963).

[40]R. Latter, Phys. Rev. 99, 510 (1955).

[41]K. Schwarz, Phys. Rev. B 5, 2466 (1972).

[42]V. O. Kostroun, M. H. Chen, and B. Crasemann, Phys. Rev. A 3, 533 (1971).

[43]M. H. Chen, B. Crasemann, and V. O. Kostroun, Phys. Rev. A 4, 1 (1971).

[44]B. Crasemann, M. H. Chen, and V. O. Kostroun, Phys. Rev. A 4, 2161 (1971).